Trends of hydroclimatic intensity in Colombia

Oscar J. Mesa[1], Andrés Ochoa[1], and Viviana Urrea[1]

[1]Universidad Nacional de Colombia

November 23, 2022

Abstract

Prediction of changes in precipitation in upcoming years and decades caused by global climate change associated with the greenhouse effect, deforestation, and other anthropic perturbations is a practical and scientific problem of high complexity and consequences. To advance toward this challenge, we look at the daily historical record of all available rain gauges in Colombia and at the CHIRPS database of daily precipitation fields to estimate the HY-INT index of the intensity of the hydrologic cycle (missing citation). The index is the product of precipitation intensity and dry spell length. Theoretical reasons indicate that global warming should lead to increasing trends in either factor or both. Most of the gauges and pixels do not show a significant trend. Nevertheless, among gauges and pixels with significant trends, the majority (70\%) exhibit a decreasing trend. The geographic distribution of results does not agree between gauges and CHIRPS. We obtain a majority of increasing trends among the 10\% of the stations and 13\% of the CHIRPS pixels with a statistically significant trend for total annual precipitation. This result agrees with previous reports. The sign of the trends for rainfall intensity, number of wet days, the average and maximum length of wet runs is opposite between the two data sets. A possible explanation is the space coverage of the two datasets. There are very few rain gauges in the eastern part of the country, and CHIRPS, with total coverage, shows an East-West dipole in the trends of those variables.

References

Trends of hydroclimatic intensity in Colombia

Oscar Mesa[1*], Viviana Urrea[1†] and Andrés Ochoa[1‡]

[1]Departamento de Geociencias y Medio Ambiente, Universidad Nacional de Colombia

Key Points:

- Precipitation trends
- Climate change
- Colombia

*Departamento de Geociencias y Medio Ambiente, Universidad Nacional de Colombia, Carrera 80 # 64-223, 050041 Medellín, Colombia

†Departamento de Geociencias y Medio Ambiente, Universidad Nacional de Colombia, Carrera 80 # 64-223, 050041 Medellín, Colombia

‡Departamento de Geociencias y Medio Ambiente, Universidad Nacional de Colombia, Carrera 80 # 64-223, 050041 Medellín, Colombia

Corresponding author: Oscar Mesa, ojmesa@unal.edu.co

Abstract

Prediction of changes in precipitation in upcoming years and decades caused by global climate change associated with the greenhouse effect, deforestation, and other anthropic perturbations is a practical and scientific problem of high complexity and consequences. To advance toward this challenge, we look at the daily historical record of all available rain gauges in Colombia and at the CHIRPS database of daily precipitation fields to estimate the HY-INT index of the intensity of the hydrologic cycle (Giorgi et al., 2011). The index is the product of precipitation intensity and dry spell length. Theoretical reasons indicate that global warming should lead to increasing trends in either factor or both. Most of the gauges and pixels do not show a significant trend. Nevertheless, among gauges and pixels with significant trends, the majority (70%) exhibit a decreasing trend. The geographic distribution of results does not agree between gauges and CHIRPS. We obtain a majority of increasing trends among the 10% of the stations and 13% of the CHIRPS pixels with a statistically significant trend for total annual precipitation. This result agrees with previous reports. The sign of the trends for rainfall intensity, number of wet days, the average and maximum length of wet runs is opposite between the two data sets. A possible explanation is the space coverage of the two datasets. There are very few rain gauges in the eastern part of the country, and CHIRPS, with total coverage, shows an East-West dipole in the trends of those variables.

1 Introduction

Predicting the effect of climate change on Colombia's hydrology, specifically precipitation, is not a small matter. To illustrate, only in the electricity sector recent studies for the Colombian Mining and Energy Planning Unit Macías and Andrade (2014) estimate that the impacts of the decrease in precipitation imply an increase in annual investment of US$ 290 million per year for the period 2013-2015. The explanation for this increase in investments is that hydroelectric generation meets approximately 70% of the country's electricity demand. We will show that this alleged declining trend obtained from models does not correspond with observations.

However, not only the impact is of magnitude, but the scientific problem of such prediction is also very complex, climate models are not necessarily accurate concerning tropical precipitation. The focus of this work is the impact of climate change on precipitation. However, global change impacts many more aspects such as temperature, sea level, coastal erosion, páramo ecosystem loss, vector-borne diseases, biodiversity, agriculture, and others.

In addition to the complexity of rainfall fields and tropical climate in the rough topography derived by the Andes cordillera, rainfall records in Colombia are generally scarce, both because of their quality, missing data, length of the records, and spatial coverage. Therefore, it is a unique challenge for Hydrology to predict the impact of climate change over Colombia rainfall on spatial and temporal scales that are suitable for critical applications. Among those applications, one can mention two very crucial, planning for the sustainable development of the territory and its hydraulic resources, and disaster prevention. Among the critical theoretical questions, one can mention the need for a better knowledge of the influence of global warming on macro-climatic phenomena like El Niño-Southern Oscillation (ENSO). In turn, a better understanding may allow better predictions. Toward that broader problem, this paper focuses on observations analysis, a necessary first step. We first present a brief review of previous work, followed by a description of the data and the methods. The remaining of the paper presents and discusses the results.

2 Previous work

This short review has two parts. First, we present the main results of previous studies about climate change impact on Colombian rainfall trends. Then we briefly show the general context of how global warming impacts precipitation.

2.1 Colombian rainfall trends

Various works describe the climatology of the precipitation in Colombia (Snow, 1976; Oster, 1979; Eslava, 1993; Mesa et al., 1997; Mejía et al., 1999; Urrea et al., 2019). The central control is the passage, twice a year, of the Inter-Tropical Convergence Zone that marks the rainy seasons of April-May and September-November in the Andes, and the seasons with the lowest rainfall in December-February and June-August. The spatial distribution of precipitation is controled by the sources of humidity in the Caribbean, the Pacific, and the Amazon, by the topography and prevailing winds. Three low-level jets play a significant role, namely the Caribbean, Chocó and the along with the easter Andes South America jet. The inter-annual variability is controlled mainly by ENSO's phenomenon in the tropical Pacific (Poveda & Mesa, 1997; Poveda et al., 2011).

Several studies have found evidence of climate change in Colombia using various statistical techniques with different record lengths (Smith et al., 1996; Mesa et al., 1997; Quintana-Gomez, 1999; Vuille et al., 2003; Ochoa & Poveda, 2008; Pabón, 2009; Cantor & Ochoa, 2011; Cantor, 2011; Carmona & Poveda, 2014; Hurtado & Mesa, 2015). In summary, these studies identify increasing mean and minimum temperature records in a significant number of stations. Besides, they find mixed trends in precipitation, with a similar percentage of stations for each trend and 20% without a statistically significant trend for the set of considered series of up to 40 years of records. For precipitation stations with longer records, the majority (63%) shows an increasing trend and only a 16% decreasing trend. There is no clear geographical pattern in the areas with a particular trend, except in the Pacific plain, which has the highest definite upward trend. The explanation for this Pacific trend may come by an increasing trend of the influence of moisture in the Pacific and the Chocó Jet. These conclusions coincide with the Colombian Meteorological Service (IDEAM) report, Mayorga et al. (2011), who analyzed 310 rainfall stations with monthly records in the period 1970-2010 using the standardized method RCLIMDEX (Peterson, 2005). They found 71 % stations with increasing trend, 22 % decreasing trend, and 7 % without a trend.

The observed trends may be due to other causes besides increasing greenhouse gas global warming: deforestation and urbanization, among others, not to mention observational issues. Concerning the impact of deforestation, Salazar (2011) estimates through a numerical experiment that a possible drastic future change in coverage in the Amazon area would bring about a reduction in precipitation in Colombia of an order of magnitude of 300 mm/year.

The warming of the Colombian Andes has led to the complete extinction of eight tropical glaciers, and the six remaining snow-caps lose ice at accelerated rates (Rabatel et al., 2013). The páramos, unique and strategic ecosystems to supply water to several cities, including Bogotá and Medellín, are also in danger by warming and other anthropogenic activities (D. Ruiz et al., 2008).

Mesa et al. (1997); Carmona and Poveda (2014) report that a large proportion of the river flow series in the Magdalena-Cauca basins have decreasing trends. Whereas, 0 to 34% of the analyzed streamflow gauges show an increase. The positive regional trend for the Atrato and San Juan flows coincide with areas of significant increasing trends in precipitation. Besides precipitation, trends in river flows may come from evapotranspiration changes.

Hurtado and Mesa (2015) developed a reanalysis of the precipitation field in Colombia, comprising 384 fields of monthly precipitation in the period 1975-2006 at a spatial resolution of 5 minutes of arc. The reanalysis used records of 2270 rain gauges and various satellite-derived products for the most recent period. Then using Empirical Orthogonal Functions, Principal Component Analysis, and statistical tests, they looked for changes or trends. According to their results, the Mann - Whitney mean change test and the simple t trend test indicate increasing precipitation trends mainly in the Pacific, Orinoco, and Amazon regions. In most of the Andean region, there are no changes or trends.

J. F. Ruiz (2010) and Pabón (2005) analyze the results of the low-resolution global climate models (GCM's) to conclude that "annual precipitation would be reduced in some regions and would increase in others". The majority of IPCC models predict an increase of around ten % for precipitation over Colombia, except the northernmost zone. The general trends of the individual models or scenarios agree in sign, although the magnitudes vary. Using downscaling of GCM's IDEAM-Colombia (2010) predicted decreasing trends that would imply a reduction of precipitation of 20% at the end of the century for many parts of the country. Later IDEAM-Colombia (2015), this prediction changed to increasing trends throughout most of the country except for the Caribbean region and the southernmost part of the Amazon region, where the prediction remained for a decreasing trend.

Concerning higher time resolution extreme precipitation, Urán (2015) carried out an analysis of the scaling between precipitation and temperature limited by the Clausius-Clapeyron using 86 stations of precipitation and nine temperature stations over the Antioquia region of Colombia, with 15 minutes resolution. He also used rain derived from TRMM data (Tropical Rainfall Measure Mission) with rainfall intensities every 3 hours. He found that for temporal scales larger than 12 hours, the trends are no longer significant. For the finer temporal scales, trends become significant for extreme deciles of the distribution. He reports a close scaling due to the Clausius-Clapeyron relation limiting the intensification of precipitation following the ideas of O'gorman and Schneider (2009).

2.2 Impact of global warming on precipitation

In response to global warming, the hydrological cycle also changes. A warmer atmosphere means more radiative cooling of the troposphere, which is a growing function of temperature. The highest infra-red radiation emission corresponds to the balance required to compensate for the larger radiation absorbed. Changes in precipitation may occur depending on the extent to which water vapor changes in cloudiness or the absorption of radiation offsets the necessary radiative cooling. Regionally, the winds determine where there is an increase or a decrease. If the winds change little, compared to the humidity they transport, the wet regions import more water, and there could be more rain, while the dry ones could be drier (Mitchell et al., 1987; Soden & Held, 2006; Wentz et al., 2007).

Giorgi et al. (2011) introduce a new measure of hydroclimatic intensity (HY-INT), which integrates metrics of precipitation intensity and dry spell length. The responses of these two metrics to global warming are deeply interconnected. They found clear increasing trends of HY-INT in global and regional climate models. The increase in HY-INT could be due to an increase in precipitation intensity, dry spell length, or both, depending on the region. They also examined late-twentieth-century observations and concluded that they also exhibit dominant positive HY-INT trends, providing a hydroclimatic signature of late-twentieth-century warming. Precipitation intensity increases because of increased atmospheric water holding capacity. However, increases in mean precipitation need increases in surface evaporation rates, which are lower than for atmospheric moisture. Global warming increases potential evaporation, which, if adequate moisture is available, may increase actual evapotranspiration in plants. Potentially, there is more drying, but in drought situations, part of any extra energy goes into increasing temperatures, thereby amplifying warming over dry land. This feedback reduces the number of wet days and an increase in dry spell length.

3 Study area and data

We analyzed precipitation data both from rain gauges and the CHIRPS database. The gauges are in 1706 sites in the whole territory of Colombia, 1062 in the Andes region. The other sites are in the Amazon, the Caribbean, the Orinoco, and the Pacific regions (respectively 77, 398, 91, and 78 stations). Data comprise daily time series of rainfall amounts. Since the method requires no missing data (Section 4) we trim the series to the shared period between 1981 and 2013. The main reason for choosing this period is the availability of data and the compromise for the objectives of having the longest possible record and the largest number of gauges covering the whole country. Figure 1 shows the IDEAM's rain gauge network. The network covers a range of elevations from sea level in the Caribbean and Pacific coasts to 4150 meters above sea level in the Andes. Notice also the low density of the gauge network in the Amazon and Orinoco regions.

The Climate Hazards Group InfraRed Precipitation with Station data (CHIRPS) is a rainfall dataset at 0.05° resolution based on satellite imagery and in-situ station. The satellite data is infrared cold cloud duration. For Colombia, they used 3,380 stations. It is, therefore, a gridded rainfall field with daily time resolution. It covers the whole country from 1981 to 2018 (Funk et al., 2015). In that paper, Funk et al. (2015) present a validation of all the dataset used against rain gauges observations in Colombia for the primary rainy season (September-November) for each year. They found a correlation between CHIRPS and the average of 338 IDEAM stations of 0.97, and a mean absolute error of 38 mm. Besides, the authors tested the performance of CHIRPS in Colombia in previous studies using further metrics and found satisfactory results (Urrea, 2017; Urrea et al., 2016). We fill the missing data in the gauge records with data from the CHIRPS dataset. A condition for this filling was that the percentage of missing days for any year did not exceed 30%. Otherwise, the whole year is missing. This decision to fill missing data is due to the small number of stations that would result if any missing day drops the whole year. Of the original IDEAM dataset, we dropped all the stations, with more than 50% missing data in the common period. Of the 1706 gauges, we filter out those having fewer than 30 years of complete record in the 33 years of the chosen period. The resulting base dataset has 909 rain gauges, but to test this filter criterion, we considered four other sensibility alternatives: the first sensibility dataset has 355 stations with no missing data in the whole record; the second sensibility dataset has 1345 stations with at least 25 years with no missing data; the third sensibility dataset has 1320 stations with at least 30 years of complete record in the chosen period but relaxing the condition for using CHIRPS data to fill any number of missing days; and finally, the fourth sensibility dataset has 1629 stations with any number of full years in the period 1970-2014 and using the 30% criteria for filling voids using CHIRP data. These sensibility alternatives seek to cover both broader and stricter criteria. We will see that the main results remain for those four.

Colombian climate is tropical, mean annual temperature is high, above 25°C at sea level, the diurnal range of temperature exceeds the annual range, and the annual range is minimal, less than 5°C (Snow, 1976). Precipitation is abundant compared to any other place in the world, mean annual 2830 mm over the whole country. There are places of the Pacific coast with perennial rain with mean annual totaling 12200 mm, the average over the region is 5010 mm. Over the Orinoco and Amazon basins in Colombia, the mean annual precipitation varies from 2000 to 7000 mm per year. The average is of the order of 1500 mm on the Caribbean coast, but to the north, there are places with near 300 mm/year. In the Andean region, the mean annual precipitation ranges from 1000 to 3000 mm/year.

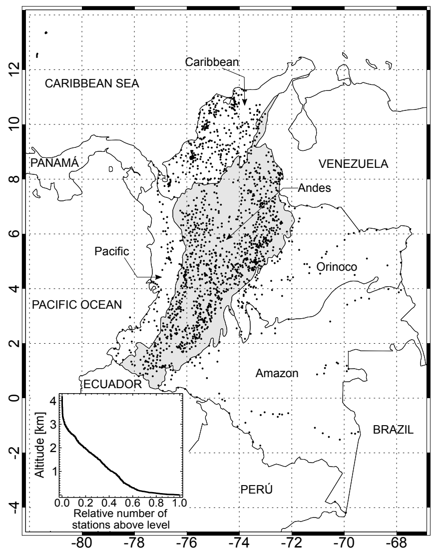

Figure 1. The points mark the location of the IDEAM rain gauge network used in this work. The bottom left graph shows the vertical distribution of the rain stations. The map also shows the five natural regions of Colombia (IGAC, 1997).

See Supporting Information figures S1 to S7 for maps of the averages of annual precipitation and the other variables considered in this study.

Atmospheric moisture is transported toward Colombia by the trade winds from the Caribbean sea, from the Atlantic ocean through both Amazon and Orinoco basins that themselves contribute with recirculating moisture. Also, from the Pacific ocean, westerly winds contribute to the massive convergence of moisture over Colombia. The migration of the inter-tropical convergence zone and three low-level jet streams (Chocó, Caribbean, and South America) are part of the complex circulation that produces such high precipitation (Poveda et al., 2014).

4 Methods

The following HY-INT indicator

$$\text{HY-INT} = \text{INT} \times \text{DSL} \tag{1}$$

evaluates the hydroclimatic intensity (Giorgi et al., 2011), where INT and DSL are mean intensity during wet days and mean dry spell length for each year in the record. In both cases, one works with scaled variables using the respective inter-annual mean as scale factor (Giorgi et al., 2011). Therefore the long-term average of both INT and DSL is 1.

We also evaluate P's trends, the total annual precipitation for each year, and WSL, mean wet spell length in each year. We counted the number of dry days and the number of dry spells in each year. The number of wet days in a year is 365 minus the number of dry days, and therefore trends in either one are opposite. Less obvious but also true is that the number of wet equals the number of dry runs in a year, or they may differ by one, depending on the parity. For both reasons, we will only report trends of the corresponding dry variables. There are other relations between the variables that are worth remembering. Before scaling, INT equals P divided by the number of wet days; and DSL equals the number of dry days divided by the number of dry runs, similarly for WSL.

Recall that the scaling makes possible the comparison of trends across stations or pixels with different average values.

Also, to construct an extreme indicator of the hydrologic cycle generalizing (Giorgi et al., 2011) ideas, we computed the maximum daily intensity for each year (INTX) and the maximum dry spell length for each year (DSLX). Therefore, in addition to the average of the corresponding variable for each year, we take the maximum. Their product gives the HYINTX indicator of the strength of the hydrologic cycle.

For each year in the record, we computed each one of the variables mentioned above. Therefore for each gauge and pixel and each variable, we have a time series. We then proceed to evaluate the existence of trends in those time series for each gauge and pixel.

4.1 Trend analysis

We use the Mann-Kendall test (Mann, 1945; Kendall, 1955) for autocorrelated data (Hamed & Ramachandra-Rao, 1998) to evaluate the existence of trends in the time series, and the Sen's slope estimator (Sen, 1968) for calculating the magnitude of the trend. A summary of these techniques follows. See more details in the cited references.

The Mann-Kendall test null hypothesis is that the data come from independent and identically distributed random variables (iid), and hence no long-term trend exists. When the data are iid, the statistic S

$$S = \sum_{i=1}^{n-1} \sum_{j=i+1}^{n} \operatorname{sgn}(x_j - x_i), \tag{2}$$

has asymptotic normality with mean zero and variance

$$\operatorname{Var}[S] = \frac{n(n-1)(2n+5)}{18} - \frac{1}{18} \sum_{j=1}^{m} t_j(t_j - 1)(2t_j + 5). \tag{3}$$

In Eq. 2, n is the sample size, x_t is the value of the time series at time t, and $\operatorname{sgn}(x_j - x_i)$ is defined by

$$\operatorname{sgn}(x_j - x_i) = \begin{cases} 1 & \text{if} \quad x_j - x_i > 0, \\ 0 & \text{if} \quad x_j - x_i = 0, \\ -1 & \text{if} \quad x_j - x_i < 0. \end{cases} \tag{4}$$

The sum in the last term of Eq. 3 accounts for the reduction in variance due to the existence of tied ranks (Hamed, 2008). In Eq. 3, m is the number of groups of tied ranks and t_j is the number of ranks in group j.

The standardized test statistic Z is calculated by

$$Z = \begin{cases} \frac{S-1}{\sqrt{\operatorname{Var}[S]}} & \text{if } S > 0, \\ 0 & \text{if } S = 0, \\ \frac{S+1}{\sqrt{\operatorname{Var}[S]}} & \text{if } S < 0. \end{cases} \tag{5}$$

The null hypothesis of no trend is rejected if $|Z|$ exceeds the value $|Z_{1-\alpha/2}|$ of the standard normal distribution for a given significance level α.

The result of the Mann-Kendall test is sensitive to autocorrelation in the data. The existence of positive autocorrelation increases the probability of false rejection. On the other hand, negative autocorrelation increases the probability of false positive. This effect occurs because of a bias in the estimation of Var$[S]$. Hamed and Ramachandra-Rao

(1998) suggested the empirical formula in Eq. 6 for calculating Var[S] in the presence of autocorrelation.

$$\mathrm{Var}[S_{ac}] = \mathrm{Var}[S] \times \left[1 + \frac{2}{n(n-1)(n-2)} \sum_{i=1}^{n-1} (n-i)(n-i-1)(n-i-2)\rho_s(i)\right], \quad (6)$$

where $\rho_s(i)$ is the auto-correlation function of the ranks of the observations.

Sen's non-parametric method (Sen, 1968) estimates the long-term linear trend slope of a time series as the median value of the slopes between all pairs of points in the series. For $N = n \cdot (n-1)/2$ pairs of data in the series, the N slopes, Q_i, are calculated as shown in Eq. 7. The median of the Q_s's is the Sen's slope estimator.

$$Q_i = \frac{x_j - x_k}{j-k}, \quad i = 1, 2, \ldots N; \quad 1 \le j \le n-1; \quad j \le k \le n. \quad (7)$$

4.2 The HY-INT trend

Even though HY-INT is not a linear function of INT and DSL, the long-term trend slope of HY-INT is a function of the trend slopes of INT and DSL. Equivalently, one can estimate it from the time series of HY-INT. Taking the time derivative of Eq. 1 one gets

$$\frac{d\text{HY-INT}}{dt} = \text{INT}\frac{d\text{DSL}}{dt} + \text{DSL}\frac{d\text{INT}}{dt}. \quad (8)$$

And because all the variables are scaled, what one needs is the logarithmic derivative

$$\frac{1}{\text{HY-INT}}\frac{d\text{HY-INT}}{dt} = \frac{1}{\text{DSL}}\frac{d\text{DSL}}{dt} + \frac{1}{\text{INT}}\frac{d\text{INT}}{dt}. \quad (9)$$

Therefore the temporal trend slopes satisfy

$$m_{HY-INT} = m_{INT} + m_{DSL}. \quad (10)$$

5 Results

We begin presenting the results for the rain gauges. After that, we proceed with the CHIRPS database and then proceed to their comparison. In the figures and tables, we present simultaneously results for each variable for both data sets to facilitate the comparison.

Neglecting data autocorrelation in trend analysis increases the probability of error in the Mann-Kendall test result (Kulkarni & von Storch, 1992; von Storch, 1995). We compared the results of the classic MK test and the MK test for autocorrelated data proposed by Hamed and Ramachandra-Rao (1998) in our 1629 series data set, and conclude that ignoring the auto-correlation may lead to false trends of the order of 20% of the gauges, and false no trends in of the order of 10% of the gauges.

Table S1 presents in each row the four elements of the confusion matrix for the Mann-Kendall test that does not take into account auto-correlation in comparison with the one that does. We take this last one as the correct method for the comparison. The largest error (from 18 to 25%) comes from false trends. However, there are also errors due to false no trends (from 11 to 15%). As a result, the accuracy (total number of hits) is between 60 and 71%. Thus, the recommendation is to take the series' autocorrelation into account to evaluate the significance of trends.

We also considered the possible implication of the definition of the starting date of the year. Besides the calendar year, we considered a hydrology year starting on April

1st. The idea was that the end of the calendar year might split the most extended dry spell. Because the dry season usually starts in mid-December and ends in March in Colombia. However, as shown below, the dominant fact for the rain gauges significant trends is more wet days (70%), no longer dry season. In summary, results do not depend on the anthropic definition of the year.

Figure S8 illustrates two of the 909 cases of the trend analysis. Notice the treatment of the missing years that may come for any missing day. For the Susacón gauge in the left part of the Figure, the trends in P, INT, and HY-INT are decreasing and statistically significant. However, the trend in DSL is not. For La Línea El Porvenir station on the right side of the Figure, DSL, INT, and HY-INT have significant positive trends, whereas P has an increasing non statistically significant trend.

Table 1 summarizes the results of the trend analysis for the more relevant variables computed for the 909 rain gauges in the base dataset, and the 37012 pixels in CHIRPS dataset. The first observation is that only a minority of the rain gauges show significant trends for any of the variables. Among the variables, INT shows the largest percentage of significant trends, but only reaching 21% of the stations. The least percentage is for the variable DSLX with only 10%. Similarly, a small percentage of all the CHIRPS pixels show significant trends for any of the variables. Again, for the intensity (INT), the percentage is one of the largest, reaching only around 25% of the pixels. The other is for the mean wet spell length (WSL), which has a similar percentage of significant pixels. The lowest percentage of significant pixels is for the maximum dry spell length (DSLX), with only 5%. Summarizing, the majority of the stations or pixels do not show significant trends for any of the variables analyzed.

Table 1. Basic statistical analysis for the base dataset (909 stations) and CHIRPS dataset (37012 pixels covering Colombia) of the significant trends of the different variables using the calendar year and taking into account autocorrelation: P: Total Annual Precipitation, INT: averaged scaled intensity on wet days, DSL: averaged scaled dry run length; HYI-NT=INT$\times$ DSL; N stands for number; WSL: averaged scaled length of wet runs; INTX: the maximum daily intensity; DSLX: the maximum dry run length; HY-INTX=INTX$\times$ DSLX; and WSLX: The maximum wet run length. Column symbols: % N Rej is the percentage of total stations or pixels for which the null hypothesis of no trend was rejected; % Pos/Rej is the percentage of stations or pixels with a significant positive trend.

Variable	% Rej/T	% Pos/Rej	% Rej/T	% Pos/Rej
	Rain Gauges		CHIRPS	
P	13	79	10	76
INT	21	54	25	48
DSL	17	20	10	48
HY-INT	21	33	23	38
N Wet Days	18	80	20	32
WSL	19	74	25	22
N Wet Runs	15	66	13	94
INTX	10	62	13	40
DSLX	10	31	5	47
HYINTX	10	38	9	48
WSLX	14	74	18	16

A second observation is that the extreme variables do not show a larger percentage of significant trends in comparison with the corresponding average variables: For INTX, the percentage of rain gauges is 10, compared with 21 for INT. Similarly, for DSLX, the percentage is 10, in comparison with 17 for DSL. For HYINTX, the percentage is 10, whereas, for HY-INT, it is 21. The same picture applies to the CHIRPS data, where the percentage of significant trends for the extreme variables is half the corresponding for average variables, except for WSLX, where the ratio is 14 to 19. Summarizing, statistical significant trends in extreme variables are less frequent than in average ones.

The analysis of positive and negative trends is interesting among the stations or pixels with statistically significant trends. There is a majority of increasing trends both for rain gauges and CHIRPS pixels for P, annual precipitation, and for the number of wet and dry runs; with a closer agreement between datasets for P, and less agreement for the number of runs where the corresponding positive trend percentages are 63 and 94. There is also accordance between rain gauges and CHIRPS for the majority of decreasing trends for HY-INT, HYINTX, DSL, and DSLX, though, for the last three variables, CHIRPS has a more ample majority. For the rest of the variables (INT, number of wet days, INTX, WSL, and WSLX), the prevalence is opposite between the two data sets. In all these last variables, the significant trends are positive for rain gauges and negative for CHIRPS. This discrepancy may come from a problem in the CHIRPS dataset already identified: "The use of TMPA 3B42 training data (as opposed to rain-rain-gauge observations) may increase the intercept values, causing CHIRP to overestimate the number of rainy days." (Funk et al., 2015). Their reference is to the Tropical Rainfall Measuring Mission Multi-satellite Precipitation Analysis version 7, one of the input data for the CHIRPS algorithm. Another possible explanation may be the space coverture of the two datasets. There are very few rain gauges in the eastern part of the country, and CHIRPS, total coverture, shows a dipole in the trends of those variables. Figures in the supporting information illustrate this dipole.

Only 33% of the stations and 38% of the pixels with significant trends show positive trends for HY-INT. Even though for one of its factors, INT, approximately half among the significant ones has positive trends (54% for stations and 48% for pixels). However, the explanation for the low percentage of significant HY-INT stations with positive trends is the sign of the trends in DSL (80% for stations and 52% for pixels have negative trends among significant DSL trends). Further insight comes from the histograms of the slopes of the trends in Figure S9. Therefore for Colombia's humid climate HY-INT, the indicator proposed by Giorgi et al. (2011) to measure the strength of the hydrologic cycle only makes sense partially. There seems to be a tendency for INT to increase. However, dry spells are not increasing in length significantly, not even among the small number of stations with significant trends that, on the contrary, are getting shorter for the average dry run and more so for the longest ones.

Figure S10 allows further analysis of the result about HY-INT. Notice that almost all stations and pixels with positive trend slope for HY-INT have positive trend slopes for both INT and DSL. Conversely, almost all with negative trends for HY-INT have negative trends for INT and DSL. Another interesting observation from the figure is the difference in the dispersion of the points between the two data sets. Because CHIRPS data are pixels of finite size, there is significant smoothing compared with rain gauges that are point observations and therefore capture the natural irregularity of the rainfall field.

Figure S11 shows the histograms of the trend slopes for the annual precipitation, the number of wet days, and the number of wet spells. Again, the majority of the stations do not have significant trends. However, among the significant ones, there is a majority of positive trends.

Table S2 summarizes the sensibility analysis for the different alternatives considered for selecting the rain gauges. The overall conclusion is that the main results are con-

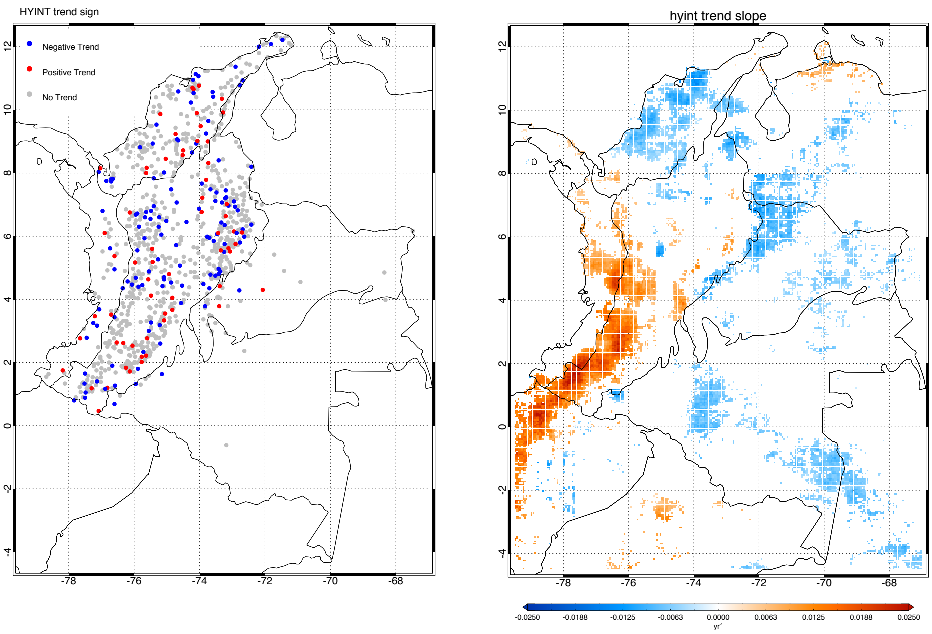

Figure 2. Maps of the trend sign for HY-INT for rain gauge base data set (left) and of the trend slope for CHIRPS data set (right). No significant trends are plotted in gray for rain gauges and not plotted for CHIRPS.

sistent among the various datasets. The base dataset is in between the alternatives. Changes in the percentage of stations with significant statistical tests for all the variables are relatively small, less than 3 points in 20. For some variables, the percentage of increasing trends among the significant trends does change more. For instance, the differences are somewhat more significant for the variables DSL, the number of dry days, WSL, DSLX, HYINTX, and INT. In general, the fourth alternative is the one with more different percentages, whereas the other three and the base dataset are close together. Recalling that that fourth alternative dataset consists of 1629 stations without consideration for the record length, one can disregard it, although it follows the general tendency of the results.

As expected from the small number of stations with significant trends, the space distribution does not seem to show any pattern. Maps in figures 2, 3, 4 and 5 show the trends in HY-INT, INT, DSL, and P. Nevertheless, the corresponding maps for the trends using CHIRPS dataset do show some space patterns, with increasing trends in the western part of the country and decreasing on the eastern side. Except for P, that has more widespread positive trends, with some small spots with decreasing trends in the south of the Pacific region, the western Amazon region, and the northern Orinoco region (figure 5). Figures S12 and S13 show the trends in the number of wet days, number of wet runs, the average length of wet runs, and the maximum length of wet runs. Trends for the number of wet days are decreasing in the west and increasing to the north and east. The number of wet runs increases almost everywhere except for some small spots to the south of the Andes. Average and maximum wet run-length decreases to the west with some weak, increasing trends to the east and north.

Table S3 shows that though the percentage of stations (13) and pixels (10) with a significant trend is small, there is a majority of positive trends for total annual pre-

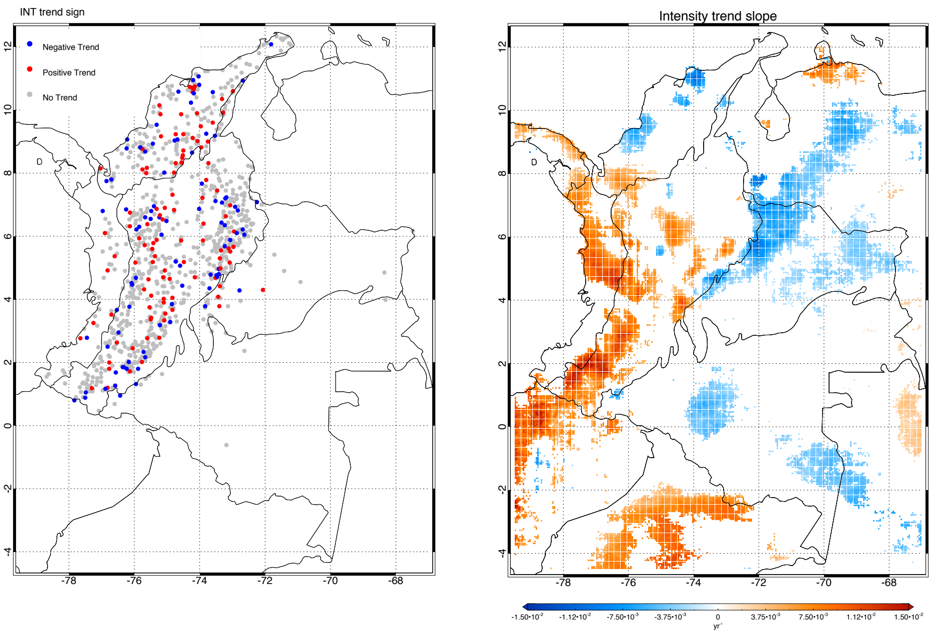

Figure 3. Maps of the trend sign for INT for rain gauge base data set (left) and of the trend slope for CHIRPS data set (right). No significant trends are plotted in gray for rain gauges and not plotted for CHIRPS.

cipitation overall (79% and 76%) and regionally. Even though the number of significant trend stations in the Pacific and Orinoco regions is minimal, and zero for the Amazon region, the CHIRPS dataset does have an ample number of pixels, with 80% positive trends for the Amazon region, 84% for the Andes, 97% for the Caribbean, 50% for the Orinoco and 76 for the Pacific region. These results accord with previous studies for the Pacific region. For the Caribbean region, the results show a trend in the opposite direction to the predictions of GCM's (see section 2).

The Pacific region exhibits some differences from the overall behavior of the country. For HY-INT, the Percentages of the stations and pixels that show statistically significant trends go up to 37 and 31% for stations and CHIRPS pixels. Nevertheless, the percentage of increasing trends among the significant ones goes from 33 and 38% for the whole country to 43 and 100%. The corresponding figures for INT, go from 54 to 67% for stations and from 48 to 100% for pixels. For DSL, only 14 stations show a significant trend, and a mere two have positive trends. However, for CHIRPS, 551 pixels have a significant trend, and 99% of those are increasing trends. The percentage of increasing significant trends for the number of wet spells goes from 66 to 80 and from %94 to 100%. For the number of wet days, the percentage of significant positive trends is 32 and 0%, whereas overall is 58 and 32%. Together with the observation about total annual precipitation, these changes indicate that the region tends to be more humid.

For the Caribbean region, another significant finding besides the increasing trends in P mentioned above is that the significant trends for HY-INT and HY-INTX are mostly decreasing, something more evident in the CHIRPS database. This decreasing trends contrast with the Pacific and Andean regions and agree with the Amazon and Orinoco regions. This contrast between the western and eastern parts of the country seems to obey a space pattern.

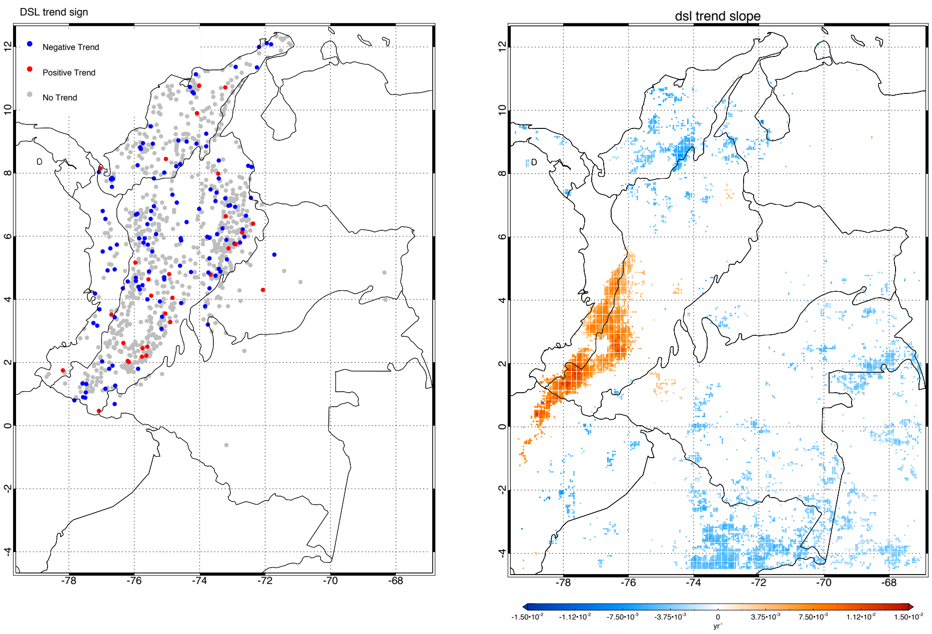

Figure 4. Maps of the trend sign for DSL for rain gauge base data set (left) and of the trend slope for CHIRPS data set (right). No significant trends are plotted in gray for rain gauges and not plotted for CHIRPS.

The Andes region has a substantial number of stations in the country, and therefore, each trend's behavior is close to the country's, except for the number of wet spells. For HY-INT, the predominant trend is increasing for the region, whereas the whole country is decreasing, dominated by the large extension of the Caribbean, Amazon, and Orinoco regions. Both components of HY-INT, INT, and DSL show predominant increasing trends too. Whereas the wet days' number decreases in the CHIRPS dataset for the region, the number of wet runs increases, with decreasing average and maximum length. The decrease in the length of wet runs is consistent with both trends in the number of wet days (numerator decreasing) and the number of runs (denominator increasing). As mentioned above, the average dry spell length (DSL) increases for the CHIRPS dataset, whereas decreases for the rain gauges. Trends for the number of dry days also increases for CHIRPS and decreases for the stations. The number of dry runs increases for both datasets.

For the Amazon and Orinoco regions, there are very few stations and even fewer significant ones. For that reason, we focus on the CHIRPS dataset results. The percentage of pixels with significant trends is low, of the order of 10% for all the variables. Among the significant ones, trends for HY-INT, INT, and DSL decrease, the number of wet days and wet runs increases, and the length of wet runs slightly increases in some few spots. Among the significant trends for total annual precipitation for the Orinoco region, approximately half increases in the south of the region, and the other half decreases in the north. For the Amazon region, 80% increases, and there is a small spot of decreasing trends to the west of the region.

We also looked into the possible dependence of trend slopes on latitude, longitude, elevation, and seasonality of the annual regime of precipitation. However, there were not any pattern worth mentioning.

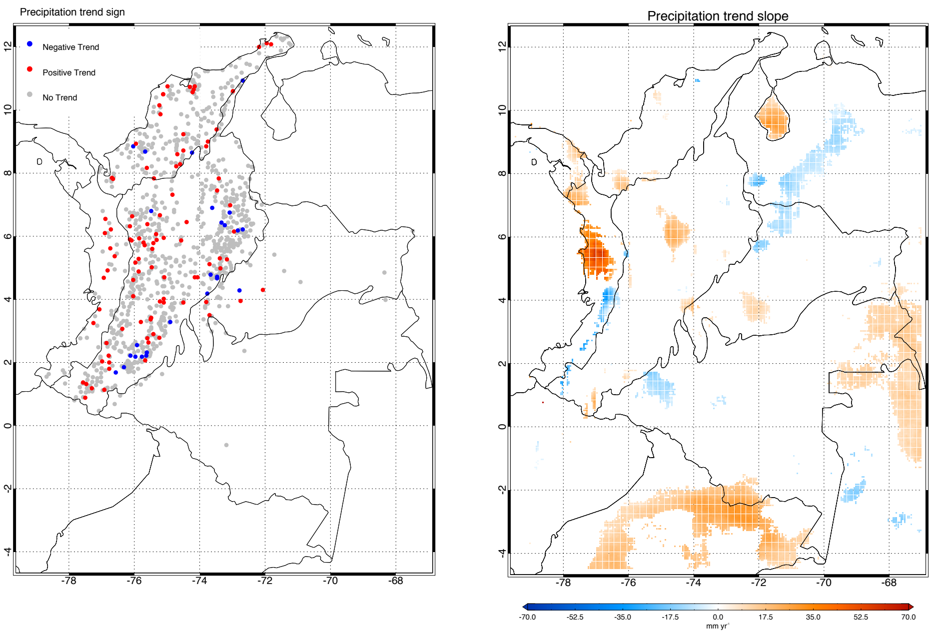

Figure 5. Maps of the trend sign for P for rain gauge base data set (left) and of the trend slope for CHIRPS data set (right). No significant trends are plotted in gray for rain gauges and not plotted for CHIRPS.

6 Discussion

Our results about the trends in annual precipitation agree in some way with the previous studies reported in Section 2 that considered rain gauges: Increasing trends prevail over decreasing trends among the statistically significant ones. However, we found a large number of stations and pixels with no significant trends.

The main result of this work is that neither the existing records of precipitation in the rain gauge network of Colombia nor the CHIRPS dataset shows a clear signal of statistically significant trends. Only approximately 20% of the gauges or pixels present significant trends. This observation is valid for all the variables we studied, even with a lower percentage of significant trends for some. Given the evidence of global climate change, this result claims for an explanation.

The humid tropical climate of Colombia is probably a factor for the explanation for the scarceness of significant trends and the sign of the found trends. Stevens and Bony (2013) has argued that changes in precipitation need changes in global circulation. The sole increase in absolute moisture is insufficient to change the amount of precipitation, at least in an average sense. In that sense, there are no reports of changes in the trade winds or the low-level jets that bring moisture to Colombia, except for the Chocó jet. This intensification of the jet is consistent with the Pacific region showing a predominant tendency to become wetter.

The lack of a space pattern for the trends in the rain gauges dataset in the Andes is another striking evidence. This lack of patterns contrasts with the results coming from the CHIRPS data set. The irregularity of the precipitation field probably plays a role because rain gauges sample the field at points. In contrast, a CHIRPS pixel data corresponds to a space average in a relatively large area (31 km^2).

The issue of changes in ENSO due to climate change is a significant area of debate Kohyama and Hartmann (2017). Some argue that ENSO could become more frequent and intense with global warming, but others that it could become weaker or more located on central rather than eastern Pacific. The effect of canonical ENSO over Colombia is to produce dryer weather, but the effect of more central ENSO is less clear. Therefore the issue is very relevant to elucidate the effects of climate change over Colombian precipitation. In that sense, our results seem to suggest that ENSO is not becoming more intense or frequent. The majority of significant trends for total annual precipitation are increasing for the Pacific region accords with the nonlinear ENSO warming suppression and possible strengthening of the Chocó jet.

The East-West dipole in the CHIRPS observed trends for the HY-INT index, intensity, the number of wet days, and the length of wet runs suggest the existence of a climate change pattern that needs confirmation, and in case it is certain deserves interpretation. Changes in ENSO impact the West part of the country more directly, whereas the Eastern part is more related to the Atlantic and Amazon basin, where other processes may be developing, see for instance Lambert et al. (2017).

Another result is about the HY-INT index of Giorgi et al. (2011) to quantify the intensity of the hydrologic cycle. For many parts of the globe, it may be true that rainfall intensity and dry spell length are deeply interconnected. However, our results suggest that it is not the case for a humid tropical climate like Colombia's. At least for the few gauges with significant trends, the two factors in the definition of HY-INT, rainfall intensity, and dry spell length do not necessarily go together. For instance, 54% (104 out of 191) of the station with significant INT trend have a positive trend; However, of those, 45% have positive DSL trends. For the 21% of CHIRPS pixels with significant trends, 62% have negative trends, mostly in the Caribbean and the eastern regions of Colombia, Amazonas, and the Orinoco. There, both INT and DSL have predominantly decreasing trends. The increasing trends are in the western part, Pacific and Andes regions, with both components, increasing. This observation points in the direction mentioned above about the dipole, the Western part of the country, with a more intense hydrological cycle.

We wanted to complement HY-INT, the indicator of the intensity of the hydrologic cycle, by defining an extreme version, HYINTX, the product of the maximum daily rainfall times the maximum dry spell length. For Colombia, this indicator did not give any good results. Even they were weaker than the original HY-INT indicator. One reason for this failure seems to be that dry spell length tends to decrease even though the maximum intensity trend is positive.

Notation

P Total annual precipitation.

Number of rainy days Number of days with precipitation larger than 1 mm.

Number of dry days Number of days with precipitation less than 1 mm=365-Number of rainy days.

Number of wet runs

Number of dry runs

INT Average intensity=P/Number of rainy days.

DSL Dry Spell Length=Average length of dry runs=number of dry days/number of dry runs

HY-INT =INT*DSL

WSL Wet Spell Length=Average length of wet runs=number of wet days/number of wet runs

INTX Maximun intensity=Maximum daily rain

DSLX Dry Spell Length=Maximum length of dry runs
HYINTX =INT*DSL
WSLX Wet Spell Length=Maximum length of wet runs

Acronyms

CHIRPS Precipitation dataset selected for the Colombian territory and whose acronym comes from Climate Hazards group Infra-Red Precipitation with Station data
IDEAM Instituto de Estudios Ambientales

Acknowledgments

Support from Universidad Nacional de Colombia is greatly acknowledged. IDEAM, the Colombian Institute for Environmental Studies provided the rain gauge records (Datasets for this research are available in http://dhime.ideam.gov.co/atencionciudadano/). CHIRPS data-set was produced by The Climate Hazards Group and U.S. Geological Survey (USGS), with support from the U.S. Agency for International Development (USAID), the National Aeronautics and Space Administration (NASA), and the National Oceanic and Atmospheric Administration (NOAA) (Datasets for this research are available in (Funk et al., 2015), also https://www.chc.ucsb.edu/data/chirps).

References

Cantor, D. (2011). *Evaluación y análisis espaciotemporal de tendencias de largo plazo en la hidroclimatología colombiana. master Thesis in Water Resources Engineering* (Master Thesis in Water Resources Engineering, Universidad Nacional de Colombia, Medellín). Retrieved from `http://bdigital.unal.edu.co/9375/`

Cantor, D., & Ochoa, A. (2011). Señales de cambio climático en series de lluvia en Antioquia. In *Ix congreso colombiano de meteorología* (p. 11 p). Bogotá: IDEAM - Universidad Nacional de Colombia. doi: 10.13140/RG.2.1.1573.0326

Carmona, A. M., & Poveda, G. (2014). Detection of long-term trends in monthly hydro-climatic series of Colombia through Empirical Mode Decomposition. *Climatic Change*, *123*(2), 301–313. Retrieved from `http://link.springer.com/10.1007/s10584-013-1046-3` doi: 10.1007/s10584-013-1046-3

Eslava, J. A. (1993). Climatología y diversidad climática de Colombia. *Revista de la Academia Colombiana de Ciencias Exactas, Físicas y Naturales*, *18*, 507–538.

Funk, C., Peterson, P., Landsfeld, M., Pedreros, D., Verdin, J., Shukla, S., ... Michaelsen, J. (2015). The climate hazards infrared precipitation with stations—a new environmental record for monitoring extremes. *Scientific Data*, *2*. doi: 10.1038/sdata.2015.66

Giorgi, F., Im, E.-S., Coppola, E., Diffenbaugh, N. S., Gao, X. J., Mariotti, L., & Shi, Y. (2011). Higher Hydroclimatic Intensity with Global Warming. *Journal of Climate*, *24*(20), 5309–5324. doi: 10.1175/2011JCLI3979.1

Hamed, K. H. (2008). Trend detection in hydrologic data: The Mann–Kendall trend test under the scaling hypothesis. *Journal of Hydrology*, *349*(3-4), 350–363. Retrieved from `http://linkinghub.elsevier.com/retrieve/pii/S0022169407006865` doi: 10.1016/j.jhydrol.2007.11.009

Hamed, K. H., & Ramachandra-Rao, A. (1998). A modified Mann-Kendall trend test for autocorrelated data. *Journal of Hydrology*, *204*(1-4), 182–196. Retrieved from `http://linkinghub.elsevier.com/retrieve/pii/S002216949700125X` doi: 10.1016/S0022-1694(97)00125-X

Hurtado, A. F., & Mesa, O. J. (2015). Cambio climático y variabilidad espacio–temporal de la precipitación en colombia. *Revista EIA*, *12*(24), 131–150.
IDEAM-Colombia. (2010). *2a Comunicación Nacional ante la Convención Marco de las Naciones Unidas sobre cambio climático*. Bogotá.
IDEAM-Colombia. (2015). *Escenarios de cambio climático para precipitación y temperatura para colombia 2011-2100.herramientas científicas para la toma de decisiones – estudio técnico completo. 3a Comunicación Nacional ante la Convención Marco de las Naciones Unidas sobre cambio climático*. Bogotá.
IGAC. (1997). *Mapa de Regiones Naturales de Colombia*. Bogotá, Colombia: Instituto Geográfico Agustín Codazzi.
Kendall, M. G. (1955). *Rank Correlation Methods* (2nd ed.). London, UK: Griffin.
Kohyama, T., & Hartmann, D. L. (2017). Nonlinear enso warming suppression (news). *Journal of Climate*, *30*(11), 4227–4251.
Kulkarni, A., & von Storch, H. (1992). Monte Carlo experiments on the effect of serial correlation on the Mann-Kendall test of trend. *Meteorologische Zeitschrift*, *4*(2), 82–85. Retrieved from `http://www.schweizerbart.de/papers/metz/detail/4/89155/Monte{\_}Carlo{\_}experiments{\_}on{\_}the{\_}effect{\_}of{\_}serial{\_}cof` doi: 10.1127/metz/4/1992/82
Lambert, F. H., Ferraro, A. J., & Chadwick, R. (2017). Land–ocean shifts in tropical precipitation linked to surface temperature and humidity change. *Journal of Climate*, *30*(12), 4527–4545.
Macías, A. M., & Andrade, J. (2014). *Estudio de generación eléctrica bajo escenario de cambio climático* (Tech. Rep.). Bogotá: Unidad de Planeación Minero Energética, UPME.
Mann, H. B. (1945). Nonparametric Tests Against Trend. *Econometrica*, *13*(3), 245–259. doi: 0012-9682(194507)13:3⟨245:NTAT⟩2.0.CO;2-U
Mayorga, R., Hurtado, G., & Benavides, H. (2011). *Evidencias de cambio climático en Colombia con base en información estadística* (Tech. Rep.). Bogotá: IDEAM–METEO/001-2011 Nota técnica del IDEAM.
Mejía, J. F., Mesa, O. J., Poveda, G., Vélez, J. I., Hoyos, C. D., Mantilla, R. I., ... Botero, B. A. (1999). Distribución espacial y ciclos anual y semianual de la precipitación en Colombia. *Dyna*, *127*, 7–26.
Mesa, O., Poveda, G., & Carvajal, L. F. (1997). *Introducción al Clima de Colombia*. Santa Fe de Bogotá, D.C., Colombia: Universidad Nacional de Colombia.
Mitchell, J. F., Wilson, C., & Cunnington, W. (1987). On co2 climate sensitivity and model dependence of results. *Quarterly Journal of the Royal Meteorological Society*, *113*(475), 293–322.
Ochoa, A., & Poveda, G. (2008). Distribución espacial de señales de cambio climático en Colombia. In *Proc. XXIII Latin American Hydraulics Meeting, IAHS, cartagena, Colombia, septembrer.*
O'gorman, P. A., & Schneider, T. (2009). Scaling of precipitation extremes over a wide range of climates simulated with an idealized gcm. *Journal of Climate*, *22*(21), 5676–5685.
Oster, R. (1979). Las precipitaciones en Colombia. *Colombia Geográfica*, *6*(2), 5–147.
Pabón, J. D. (2005). Escenarios de cambio climático para territorio Colombiano. *Documento INAPPDF-B*.
Pabón, J. D. (2009). El cambio climático global y su manifestación en Colombia. *Cuadernos de Geografía: Revista Colombiana de Geografía*, *12*, 111–119.
Peterson, T. (2005). Climate change indices. *WMO Bulletin*, *54*(2), 83–86.
Poveda, G., Álvarez, D. M., & Rueda, Ó. A. (2011). Hydro-climatic variability over the Andes of Colombia associated with ENSO: a review of climatic processes and their impact on one of the earth's most important biodiversity hotspots. *Climate Dynamics*, *36*(11-12), 2233–2249.
Poveda, G., Jaramillo, L., & Vallejo, L. F. (2014). Seasonal precipitation patterns

along pathways of South American low-level jets and aerial rivers. *Water Resources Research*, *50*(1), 98–118. doi: 10.1002/2013WR014087

Poveda, G., & Mesa, O. J. (1997). Feedbacks between hydrological processes in tropical South America and large-scale ocean-atmospheric phenomena. *Journal of Climate*, *10*(10), 2690–2702.

Quintana-Gomez, R. A. (1999). Trends of maximum and minimum temperatures in northern South America. *Journal of Climate*, *12*(7), 2104–2112.

Rabatel, A., Francou, B., Soruco, A., Gomez, J., Cáceres, B., Ceballos, J., ... Wagnon, P. (2013). Current state of glaciers in the tropical andes: a multi-century perspective on glacier evolution and climate change. *The Cryosphere*, *7*(1), 81–102.

Ruiz, D., Moreno, H. A., Gutiérrez, M. E., & Zapata, P. A. (2008). Changing climate and endangered high mountain ecosystems in Colombia. *Science of The Total Environment*, *398*(1-3), 122–132. Retrieved from `http://linkinghub.elsevier.com/retrieve/pii/S0048969708002246` doi: 10.1016/j.scitotenv.2008.02.038

Ruiz, J. F. (2010). *Cambio climático en temperatura, precipitación y humedad relativa para Colombia usando modelos meteorológicos de alta resolución. panorama 2011 – 2100* (Tech. Rep.). Bogotá: IDEAM Nota técnica 005/2010.

Salazar, J. F. (2011). *Regulación biótica del ciclo hidrológico en múltiples escalas* (Unpublished doctoral dissertation). PhD thesis. Universidad Nacional de Colombia. Medellín.

Sen, P. K. (1968). Estimates of the Regression Coefficient Based on Kendall's Tau. *Journal of the American Statistical Association*, *63*(324), 1379. Retrieved from `http://www.jstor.org/stable/2285891` doi: 10.2307/2285891

Smith, R., Poveda, G., Mesa, O., Pérez, C., & Ruiz, C. (1996). En búsqueda de señales del cambio climático en Colombia. In *Iv congreso Colombiano de meteorología, sociedad Colombiana de meteorología, bogotá.*

Snow, J. (1976). The Climate of Northern South America. In W. Schwerdtfeger (Ed.), *World survey of climatology volume 12: Climates of central and south america* (pp. 295–403). Amsterdam, Netherlands: Elsevier.

Soden, B. J., & Held, I. M. (2006). An assessment of climate feedbacks in coupled ocean-atmosphere models. *Journal of Climate*, *19*(14), 3354–3360.

Stevens, B., & Bony, S. (2013). What are climate models missing. *Science*, *340*(6136), 1053–1054.

Urán, J. D. (2015). *Cambios en los valores extremos de precipitación en regiones tropicales asociados a cambio climático.* (Unpublished master's thesis). Posgrado en Aprovechamiento de Recursos Hidráulicos. Universidad Nacional de Colombia Sede Medellín.

Urrea, V. (2017). *Variabilidad espacial y temporal del ciclo anual de lluvia en colombia* (Master's thesis, Posgrado en Aprovechamiento de Recursos Hidráulicos. Universidad Nacional de Colombia Sede Medellín). Retrieved from `http://bdigital.unal.edu.co/57578/`

Urrea, V., Ochoa, A., & Mesa, O. (2016). Validación de la base de datos de precipitación CHIRPS para Colombia a escala diaria, mensual y anual en el período 1981-2014. In *XXVII Congreso Latinoamericano de Hidráulica* (p. 11). Lima, Perú: IAHS. Retrieved from `http://ladhi2016.org/`

Urrea, V., Ochoa, A., & Mesa, O. (2019). Seasonality of rainfall in colombia. *Water Resources Research*, *55*(5), 4149-4162. Retrieved from `https://agupubs.onlinelibrary.wiley.com/doi/abs/10.1029/2018WR023316` doi: 10.1029/2018WR023316

von Storch, H. (1995). Misuses of Statistical Analysis in Climate Research. In H. von Storch & A. Navarra (Eds.), *Analysis of climate variability: Applications of statistical techniques* (pp. 11–26). Berlin: Springer- Verlag.

Vuille, M., Bradley, R. S., Werner, M., & Keimig, F. (2003). 20th century climate change in the tropical andes: observations and model results. In *Climate variability and change in high elevation regions: past, present & future* (pp. 75–99). Springer.

Wentz, F. J., Ricciardulli, L., Hilburn, K., & Mears, C. (2007). How much more rain will global warming bring? *Science*, *317*(5835), 233–235.

Supporting Information for "Trends of hydroclimatic intensity in Colombia"

Oscar Mesa[1] *, Viviana Urrea[1] † and Andrés Ochoa[1] ‡

[1]Departamento de Geociencias y Medio Ambiente, Universidad Nacional de Colombia

Contents of this file

1. Figures S1 to S12

---

*Departamento de Geociencias y Medio Ambiente, Universidad Nacional de Colombia, Carrera 80 # 64-223, 050041 Medellín, Colombia

†Departamento de Geociencias y Medio Ambiente, Universidad Nacional de Colombia, Carrera 80 # 64-223, 050041 Medellín, Colombia

‡Departamento de Geociencias y Medio Ambiente, Universidad Nacional de Colombia, Carrera 80 # 64-223, 050041 Medellín, Colombia

2. Tables S1 to S3

Introduction We analyzed precipitation data both from rain gauges and the CHIRPS database. The gauges are in 1706 sites in the whole territory of Colombia from Colombian Meteorological Service (IDEAM) rain gauge network. Data comprise daily time series of rainfall amounts. We also used the Climate Hazards Group InfraRed Precipitation with Station data (CHIRPS) (Funk et al., 2015).

Figure S1 presents a map of the mean annual precipitation over Colombia. Similar maps for the averages of the other variables considered in this study are in figures S2 to S6. Figure S7 shows the histograms of the spatial distribution of the mean annual precipitation and the mean annual number of rainy days.

Table S1 presents the confusion matrix that illustrates the need to consider the auto-correlation of the series in estimating trends for the variables of this study.

Table S2 shows a sensibility analysis of the results obtained using the different filters of the rain gauge data.

Table S3 presents a regional summary of the trends of the main variables studied.

Figure S8 shows examples of trend analysis for two stations. Figure S9 presents the histograms of the HYINT, INT, and DSL trend slopes. Similarly, Figure S11 presents the trend slope of the histograms of the total annual precipitation, the number of wet days in the year, and the number of wet spells. Figure S10 shows a dispersion diagram of the DSL trend slope vs. INT trend slope. Figures S12 and S13 present maps of the trend slope for the number of wet days, the number of wet runs, the average length of wet runs, and the maximum length of wet runs.

References

Funk, C., Peterson, P., Landsfeld, M., Pedreros, D., Verdin, J., Shukla, S., ... Michaelsen, J. (2015). The climate hazards infrared precipitation with stations—a new environmental record for monitoring extremes. *Scientific Data*, *2*. doi: 10.1038/sdata.2015.66

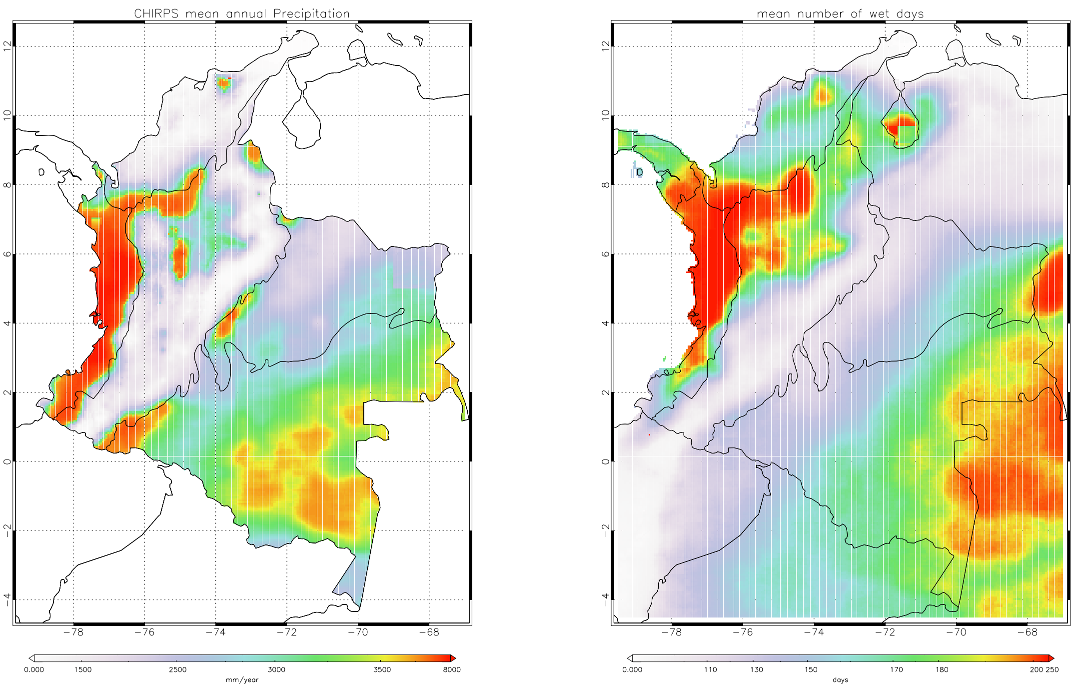

Figure S1. Mean annual precipitation over the period 1981-2018 from CHIRPS database (left). Mean annual number of rainy days over the same period (right).

Table S1. Confusion matrices for the evaluation method of the significance of the trends for each of the indicated variables without taking into account auto-correlation. For the illustration, the Mann-Kendall test with auto-correlation is considered the true one. The Table shows the results for the fourth sensibility data set, but notice the similarity among all datasets.

Variable	true trend R-R	false trend R-NR	false no trend NR-R	true no trend NR-NR
	Number of gauges (Percentage of the total number of gauges)			
P	45 (3%)	293 (18%)	180 (11%)	1111 (68%)
INT	116 (7%)	400 (25%)	245 (15%)	868 (53%)
DSL	62 (4%)	316 (19%)	184 (11%)	1067 (66%)
HY-INT	108 (7%)	393 (24%)	212 (13%)	916 (56%)

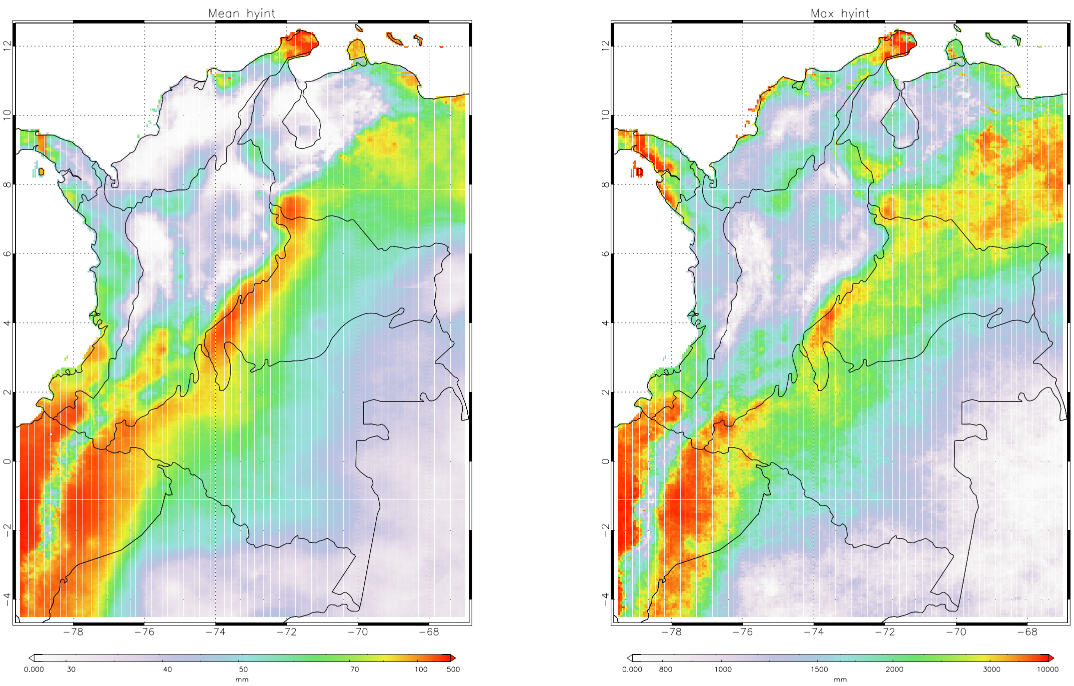

Figure S2. Average hyint over the period 1981-2018 from CHIRPS database (left). Average hyintx over the same period (right).

Table S2. Comparison of sensibility alternatives for data filtering. Percentage of stations with a significant trend for each of the four sensibility data sets (%S1 to %S4) and percentage of those with positive trends (%P1 to %P4). Variable symbols are the same as in Table 1.

Variable	%S1	%S2	%S3	%S4	%P1	%P2	%P3	%P4
N Gauges	355	1345	1320	1629				
P	12	13	14	14	80	81	82	73
INT	21	20	19	22	49	56	59	57
DSL	18	16	15	15	17	18	20	31
HY-INT	22	18	18	20	29	33	34	40
N Wet Days	18	17	17	17	74	81	80	71
WSL	20	19	17	18	83	75	74	64
N Wet Runs	17	15	14	14	66	64	62	58
INTX	11	9	10	9	68	62	64	57
DSLX	11	9	10	9	34	27	26	20
HYINTX	10	9	10	9	43	34	37	26
WSLX	17	14	14	14	77	74	71	64

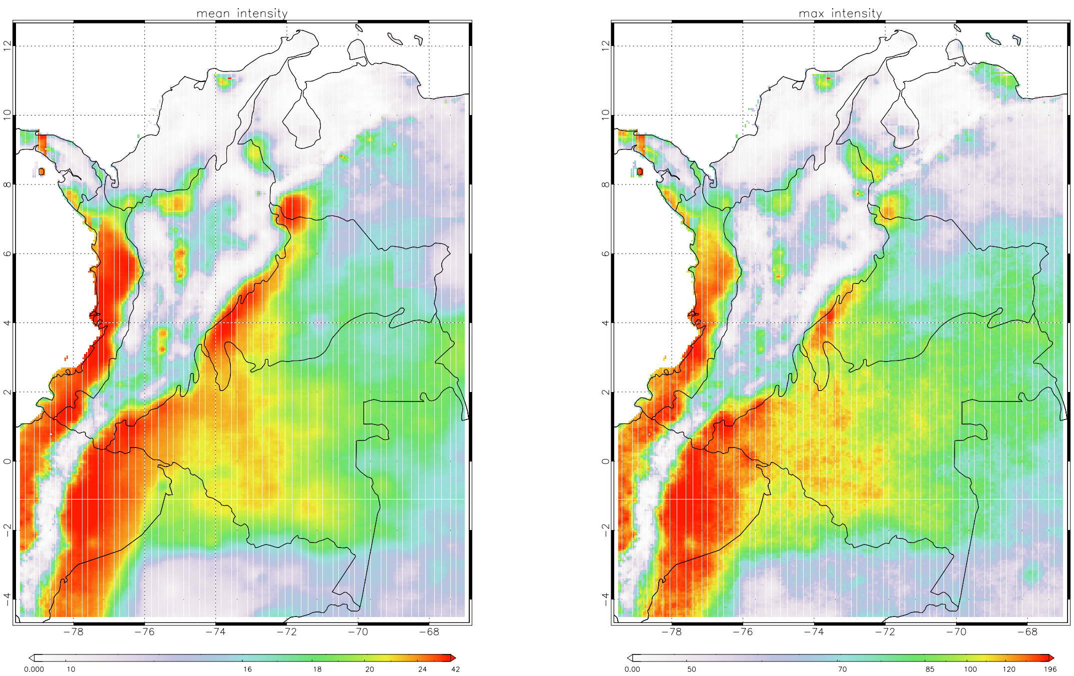

Figure S3. Mean average intensity over the period 1981-2018 from CHIRPS database (left). Mean maximum intensity over the same period (right).

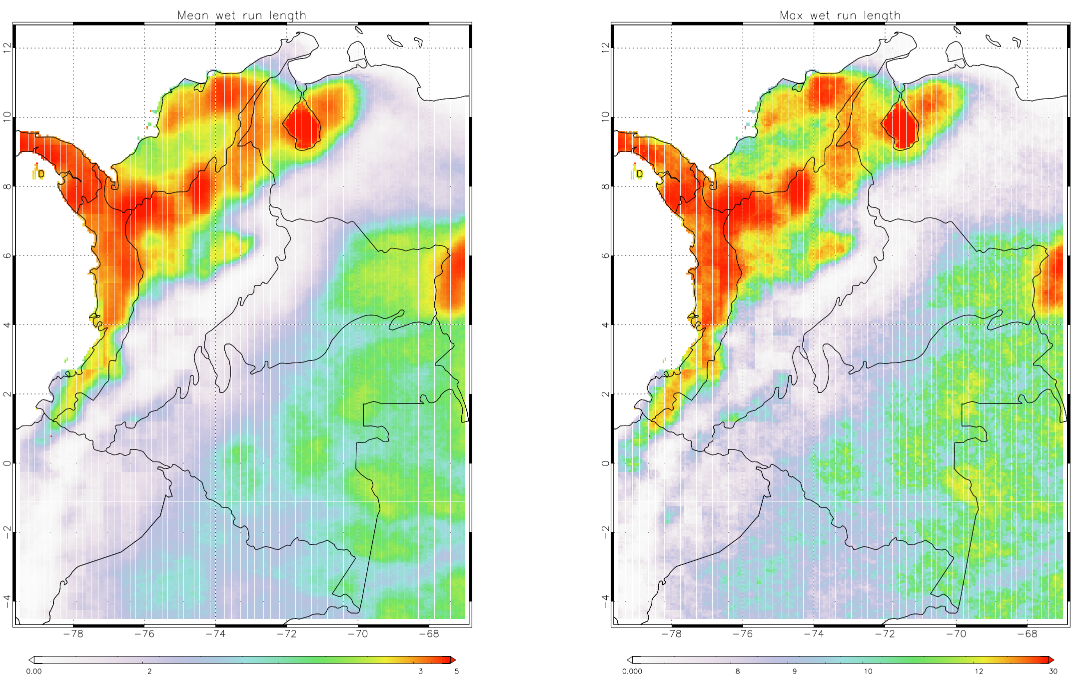

Figure S4. Mean wet run length over the period 1981-2018 from CHIRPS database (left). Mean maximum wet run length over the same period (right).

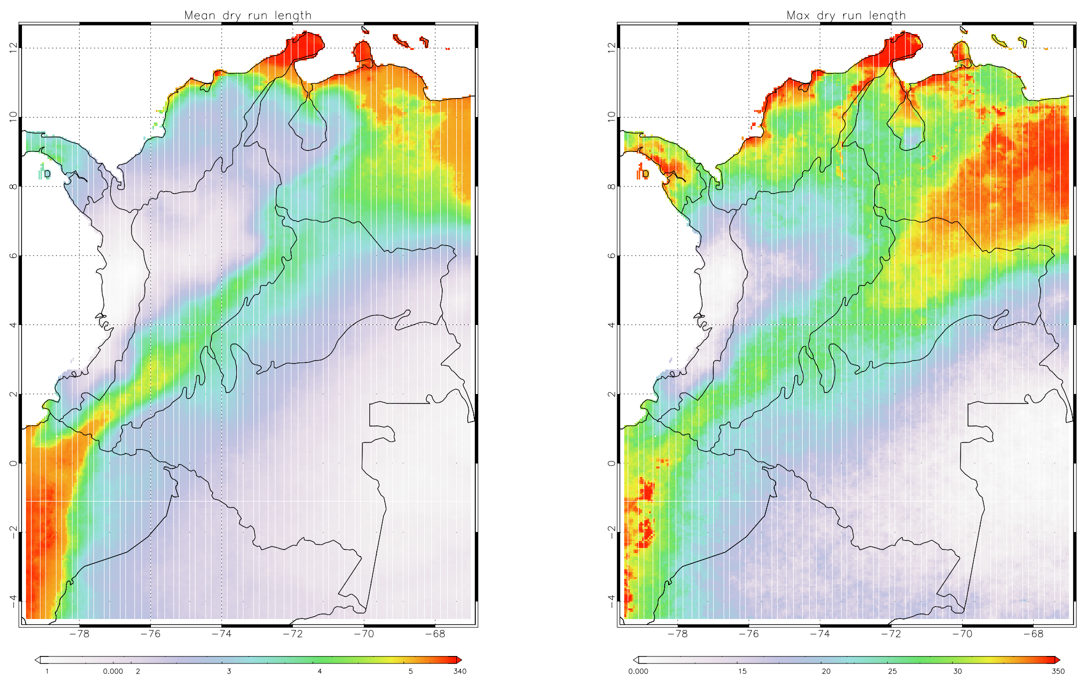

Figure S5. Mean dry run length over the period 1981-2018 from CHIRPS database (left). Mean maximum dry run length over the same period (right).

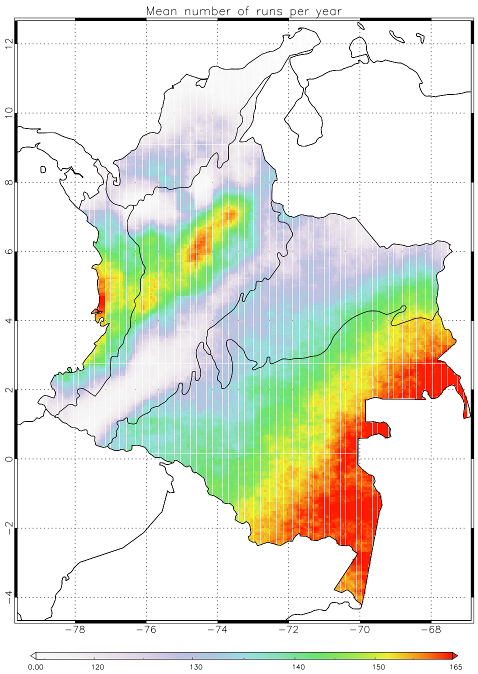

Figure S6. Mean number of runs over the period 1981-2018 from CHIRPS database

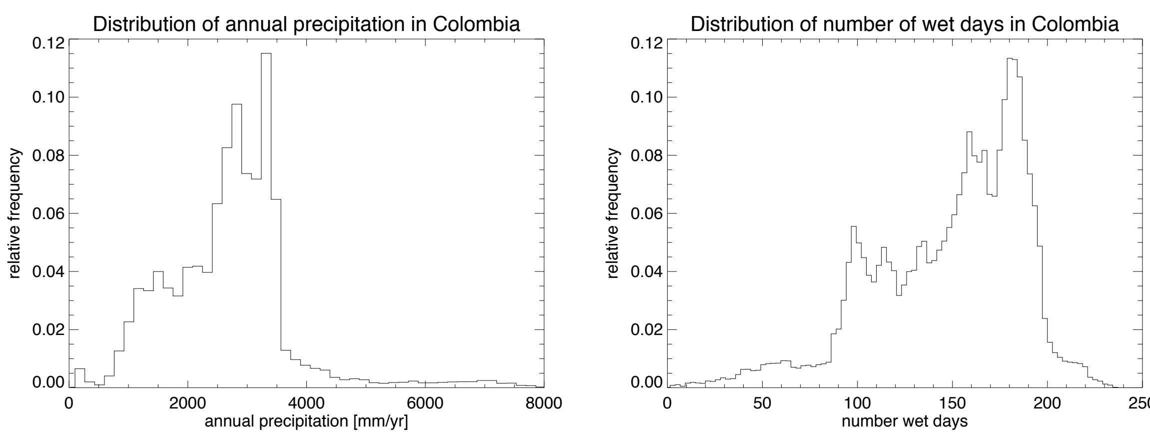

Figure S7. Histograms of mean annual precipitation over the period 1981-2018 from CHIRPS database (left) and mean annual number of rainy days over the same period (right).

Table S3. Regional summary of the trends of the base rain gauges and CHIRPS datasets for Total Annual Precipitation, HY-INT, INTX and HYINTX. Column symbols as in Table 1. The number of stations and pixels for each region are: Amazon, 12 and 14006; Andes, 622 and 9741; Caribbean, 207 and 3901; Orinoco, 30 and 6729; and Pacific, 38 and 2635 respectively

	Rain Gauges		CHIRPS	
Region	% Rej/T	% Pos/Rej	% Rej/T	% Pos/Rej
Total Annual Precipitation				
Amazon	0	-NaN	10	80
Andes	12	73	6	84
Caribbean	14	90	4	97
Orinoco	17	80	8	50
Pacific	24	100	28	76
Total	13	79	10	76
HY-INT				
Amazon	25	0	12	0
Andes	20	30	31	79
Caribbean	21	36	40	4
Orinoco	17	60	22	0
Pacific	37	43	31	100
Total	21	33	23	38
INTX				
Amazon	17	0	4	43
Andes	11	62	20	53
Caribbean	8	62	22	5
Orinoco	7	100	12	12
Pacific	8	67	17	100
Total	10	62	13	40
HYINTX				
Amazon	8	0	5	17
Andes	10	38	13	71
Caribbean	6	58	12	26
Orinoco	7	100	6	3
Pacific	24	0	15	100
Total	10	38	9	48

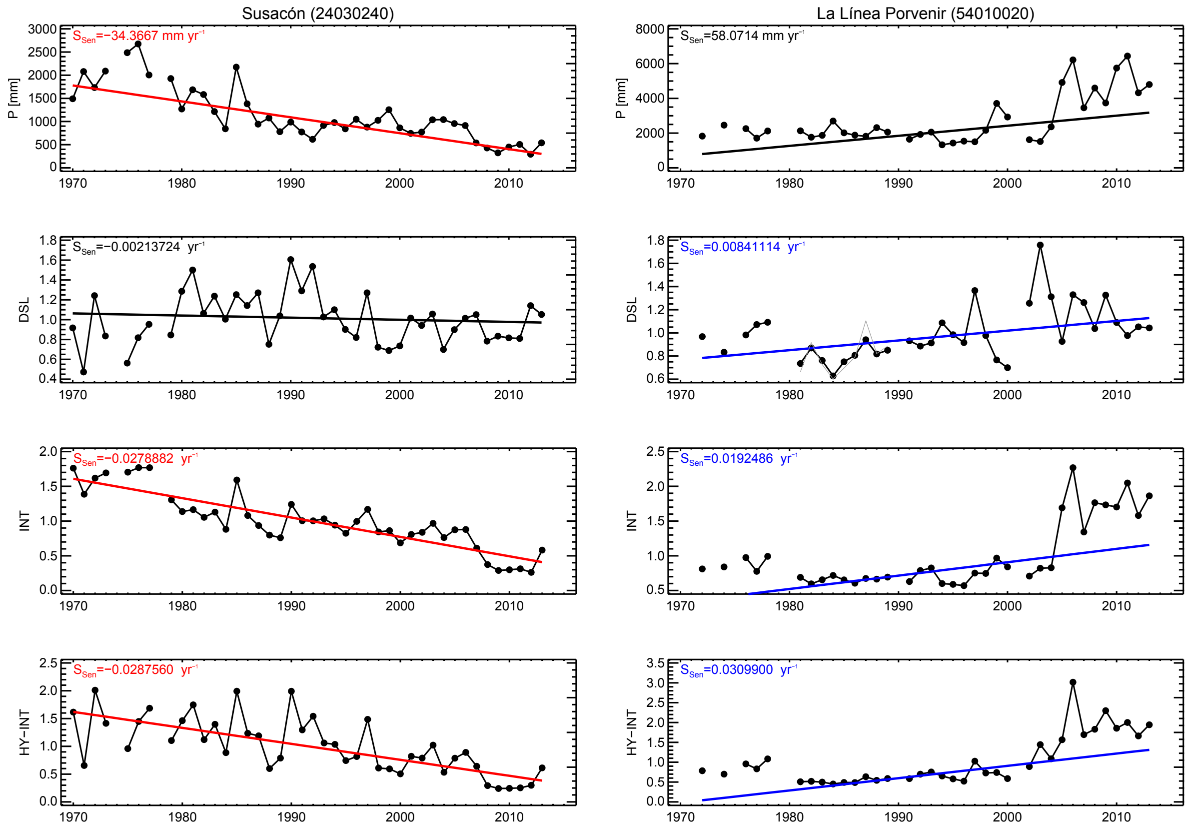

Figure S8. Two examples of trend analysis for (top to bottom) P, DSL, INT, and HY-INT for two representative stations, left panel: Susacón in Boyacá, at 2550 masl, right panel: La Línea El Porvenir in Risaralda, at 1955 masl.

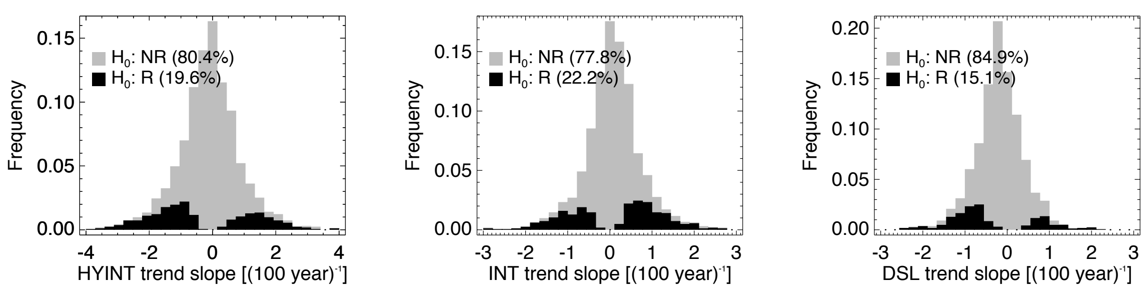

Figure S9. Histograms of the HYINT (left), INT (center), and DSL (right) trend slopes of the fourth alternative dataset. Non-significant trends (H_0: Stationary hypothesis not rejected, NR) in grey and significant trends in black (H_0: Stationary hypothesis rejected, R). Results are similar for other datasets.

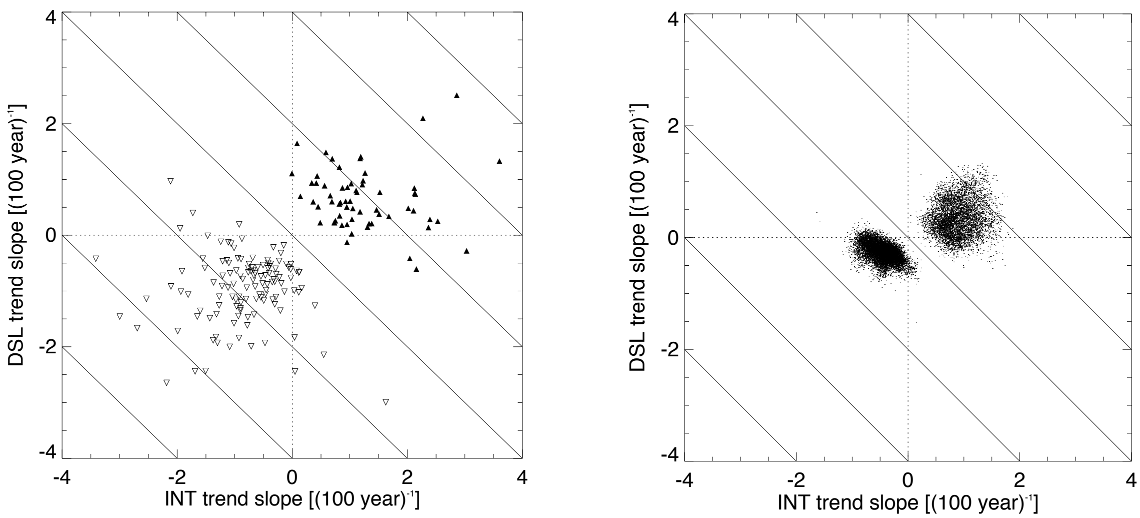

Figure S10. Dispersion diagram of the DSL trend slope vs. INT trend slope for all stations in the base dataset (left) and all pixels in the chirps dataset (right) with significant HY-INT trend slope. Notice that because of Eq 10, the trend slope of HY-INT is the sum of the trend slopes of INT and DSL. This equation explains the slanted iso-lines for the HY-INT trend slope.

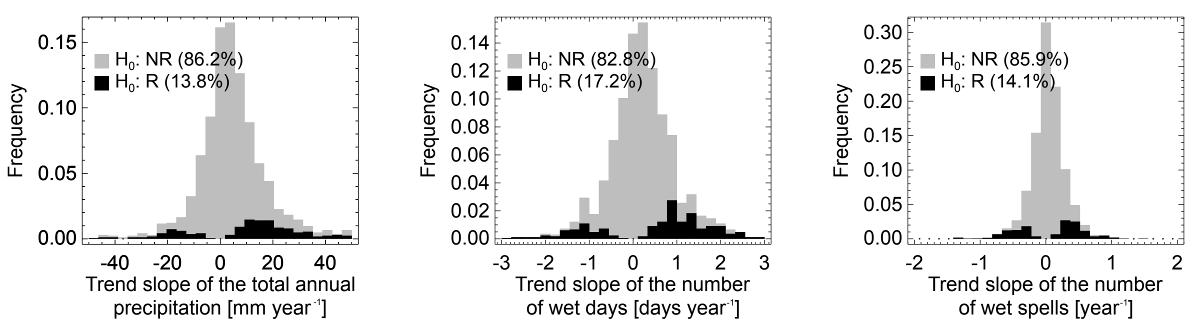

Figure S11. Same as Figure S9 for the trend slope of the total annual precipitation (left), the number of wet days in the year(center) and number of wet spells in the year (right).

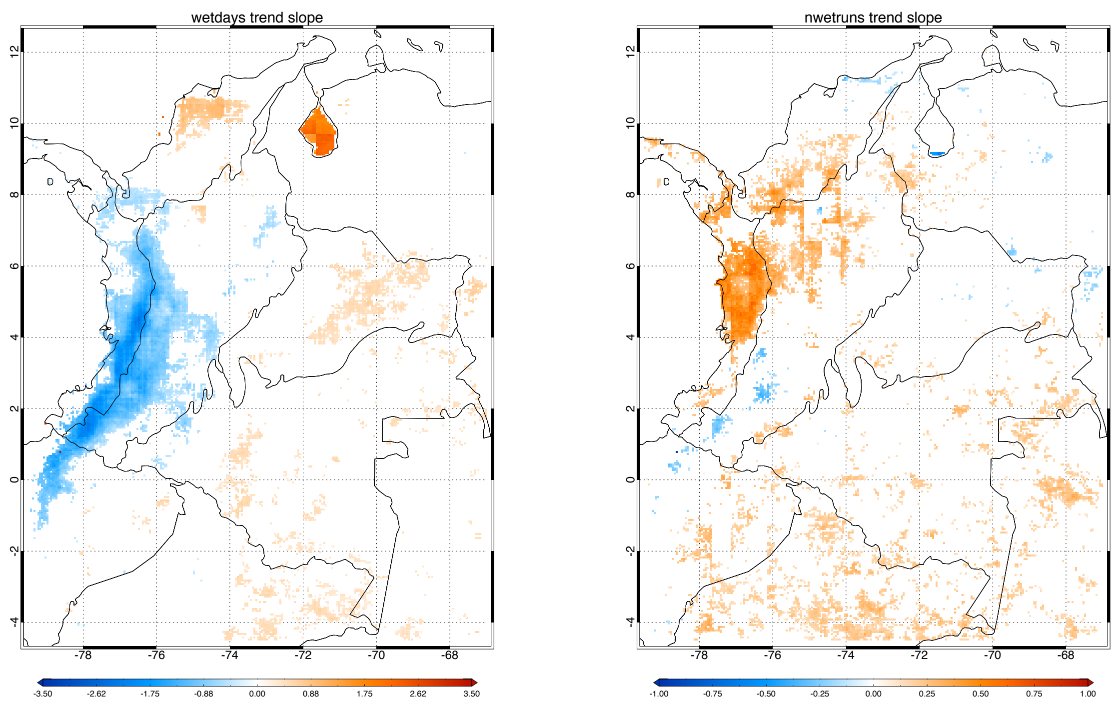

Figure S12. Maps of the trend slope for number of wet days (left) and the number of wet runs (right) for CHIRPS data set. No significant trends are not plotted.

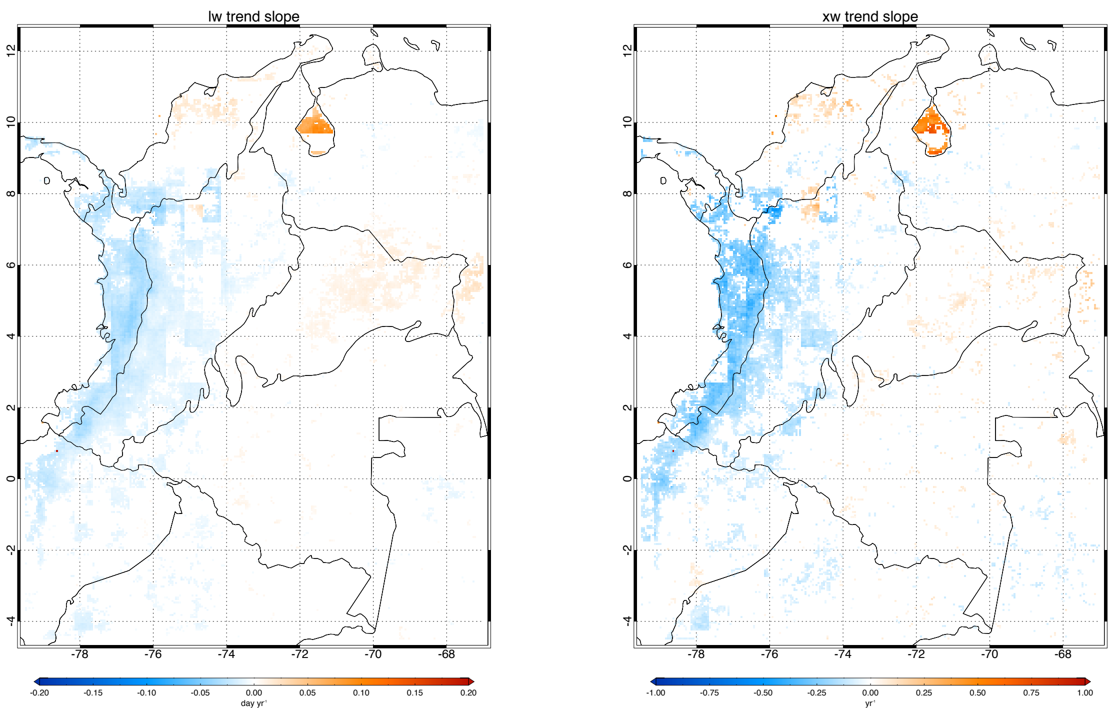

Figure S13. Maps of the trend slope for average length of wet runs (left) and the maximum length of wet runs (right) for CHIRPS data set. No significant trends are not plotted.